

Simulation Method of Microscale Fluid-Structure Interactions: Diffuse-Resistance-Domain Approach

Min Gao,¹ Zhihao Li,^{2,3} and Xinpeng Xu^{3,4,*}

¹School of General Studies, Guangzhou College of Technology and Business,
5 Guangming Road, Guangzhou, Guangdong 510850, China

²Department of Civil Engineering, Shantou University,
243 Daxue Road, Shantou, 515063, Guangdong, China

³Department of Physics and MATEC Key Lab, Guangdong Technion - Israel Institute of Technology,
241 Daxue Road, Shantou, Guangdong 515063, China

⁴Technion - Israel Institute of Technology, Haifa 3200003, Israel

(Dated: July 22, 2024)

Direct numerical simulations (DNS) of microscale fluid-structure interactions (mFSI) in multicomponent multiphase flows pose many challenges such as the thermodynamic consistency of multiphysics couplings, the tracking of moving interfaces, and the dynamics of moving triple-phase contact lines. We propose and validate a generic DNS approach: Diffuse-Resistance-Domain (DRD). It overcomes the above challenges by employing Onsager's principle to formulate dynamic models and combining traditional diffuse-interface models for fluid-fluid interfacial dynamics with a novel implementation of complex fluid-solid interfacial conditions via smooth interpolations of dynamic-resistance coefficients across interfaces. After careful validation by benchmark simulations, we simulated three challenging mFSI problems taken from different fields. This generic DNS approach offers a promising tool for understanding physical mechanisms, controlling microscale fluids, and optimizing engineering processes in microfluidics, additive manufacturing, and biomedical engineering.

Keywords: fluid-structure interactions; direct numerical simulations; microfluidics; active matter; porous-media flows

Microscale fluid-structure interactions (mFSI) refer to the complex dynamics interplay between multicomponent multiphase flows and moving, deformable, or evolving solid structures at length scales ranging typically $1 - 100 \mu\text{m}$ [1, 2]. mFSI differs from macroscale FSI in many aspects and physical effects such as viscous dissipation, interfacial tensions, wettability, and fluid slip start to dominate the system. Understanding mFSI is crucial for various applications, including microfluidics, additive manufacturing, active matter physics, biomedical engineering, geophysics, and civil engineering, *etc* [1]. However, a comprehensive study of mFSI remains a huge challenge due to the large surface-area-to-volume ratio and multiphysics multi-field couplings [3, 4]. Direct numerical simulations (DNS) are usually employed to investigate the fundamental physics involved in mFSI [2–5].

Numerous DNS methods have been developed to tackle the complexities of mFSI. These methods can be broadly classified into two types [3] – partitioned and monolithic approaches, each with its strengths and limitations. The partitioned approach treats fluids and solids as two computational fields that are solved separately and supplemented by proper interfacial conditions at fluid-solid interfaces. It integrates available models and numerical methods which have been validated for solving complicated fluid or solid problems. Examples are the immersed boundary methods [5], arbitrary Lagrangian-Eulerian method [6], and some particle-based simulation methods, *e.g.*, smoothed particle hydrodynamics method [7], dissipative particle dynamics method [8], and multi-particle collision dynamics method [9], *etc*. The

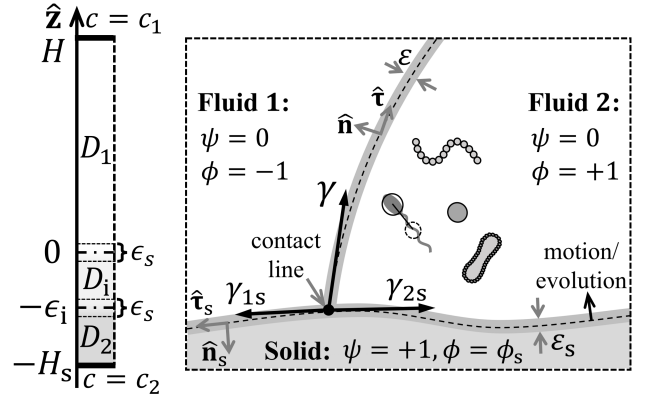


FIG. 1. Schematic illustrations of the DRD approach and its applications. (left) Demonstration and validation by solving the 1D diffusion equation for $0 \leq z \leq H$. Different boundary conditions at $z = 0$ are effectively imposed by smooth interpolations of the diffusivity D over 2 or 3 domains. (right) Applications to simulate complex mFSI where interfacial conditions are imposed effectively by smooth interpolations of dynamic-resistance coefficients in different domains.

monolithic approach treats fluids and solids in the same mathematical framework by a single set of equations simultaneously solved by a unified algorithm. Examples include multi-phase-field method [10–12], fictitious domain method [13], diffuse domain method [14, 15], smoothed profile method [16, 17], and fluid particle dynamics (FPD) method [18, 19], *etc*. There also exist some other popular methods such as lattice Boltzmann

method [20] that can be either partitioned or monolithic depending on the solved model.

Despite the development of these powerful DNS methods for mFSI, two major challenges persist. (i) *mFSI in multicomponent multiphase flows* [3]. Most above methods consider mFSI between immersed solid structures and one-component single-phase flows. mFSI in multicomponent multiphase flows is less explored and it poses significant challenges in both model construction (thermodynamic consistency) and algorithm development due to the complex multiphysics multi-field couplings. (ii) *Boundary conditions at multiple dynamic interfaces and near triple-phase contact lines* [1, 2, 21]. Due to the large surface-area-to-volume ratio at microscales, defining appropriate boundary conditions that accurately represent the physical system is essential for reliable simulations. However, this can be very challenging and computationally expensive, particularly when the interface (solid) geometry is complicated or when the interfaces are moving, deforming, or evolving due to reactions or phase transitions such as solidification and evaporation.

In this work, we propose a generic monolithic DNS approach – Diffuse-Resistance-Domain (DRD) approach, to overcome the above major challenges in simulating mFSI in multicomponent multiphase flows. In this approach, firstly, all the interfaces are treated as *diffuse* interfaces described by phase parameter fields. Secondly, thermodynamic consistency is ensured by deriving the governing equations using Onsager’s principle and linear response theory [22]: $X_i = \mathcal{R}_{ij}\dot{\alpha}_j$ with X_i and $\dot{\alpha}_i$ being the conjugate thermodynamic force-flux pair, and \mathcal{R}_{ij} being the *resistance* coefficient matrix that is symmetric and positive definite. Thirdly, in contrast to multi-phase-field methods for mFSI, the phase parameter fields for the fluid-solid interfaces are prescribed *a priori* by

$$\psi(\mathbf{r}, t) = \frac{1}{2} \left[1 + \tanh \left(\frac{\mathcal{D}(\mathbf{r}, t)}{\sqrt{2}\epsilon_s} \right) \right], \quad (1)$$

changing smoothly from the fluid domains ($\psi = 0$) to the solid domain ($\psi = 1$). Here ϵ_s is the interface thickness and $\mathcal{D}(\mathbf{r}, t)$ is the signed distance function (encoding the complicated solid geometries) away from the solid surface with $\mathcal{D} > 0$ (< 0) in the solid (fluid) domain. In this case, the phase parameter ψ does not need to evolve by Cahn-Hilliard or Allen-Cahn equations but is prescribed based on the position of the interface that moves, deforms, or evolves with known or separately-solved local velocities. The solids are regarded as domains with resistance coefficients \mathcal{R}_{ij} that have a large contrast to those of fluid domains. In this way, the governing equations already developed in sharp interface models of mFSI can be easily extended to the whole fluid-solid system by smoothly interpolating \mathcal{R}_{ij} via ψ over different domains. Moreover, in comparison to the diffuse-domain method [14], the governing equations in the DRD approach applicable to both multiphase fluids and the solid structures take

the same form as those for multiphase fluids alone, which then significantly simplifies the development of numerical algorithms.

DRD approach in a nutshell: simulating 1D diffusion

– We first explain the main components of the DRD approach and use it to solve the one-dimensional (1D) diffusion equation with three typical types of boundary conditions (see Fig. 1). We treat the fluid-solid interface at $z = 0$ as a diffuse interface described by a phase parameter function $\psi(z, t)$ in the form of Eq. (1). Then, to reproduce the boundary conditions at $z = 0$ properly, we need to take proper smooth interpolations of the diffusivity D over different domains. For the Dirichlet and Neumann boundary conditions, we can choose a simple smooth interpolation of $D(z)$ as

$$D(\psi) = D_f + (D_s - D_f)\psi, \quad (2)$$

with D_f and D_s being the diffusivity of the fluid and solid domains, respectively. In the sharp interface limit ($\epsilon_s \rightarrow 0$), if $D_s \gg D_f$, we reproduce the Dirichlet boundary condition effectively, whereas, if $D_s \ll D_f$, we would instead reproduce the Neumann boundary condition (see Fig. S2 [23]). In contrast, to reproduce the Robin boundary condition (see Fig. S3 [23]), we have to introduce the third intermediate domain of small thickness ϵ_i with a very small diffusivity D_i ($< D_f \ll D_s$) and take an interpolation of D over the three domains (see Eq. (S5) [23]).

The above idea can be easily extended to numerically solve dynamic equations of other transport phenomena, *e.g.*, heat conduction equation, Navier-Stokes equation, Cahn-Hilliard and Allen-Cahn equations, electrokinetic equation, *etc.* For example, when the only irreversible process in mFSI is the fluid-solid two-phase hydrodynamics, the DRD approach yields the FPD method [18], where the governing equation is the Navier-Stokes equation, the only relevant resistance coefficient is the viscosity, and the solid is regarded as a domain with a viscosity much larger than fluid viscosity. In this case, we only need to solve the Navier-Stokes equation with spatially varying viscosity; many efficient algorithms have already been developed and can be used directly. The FPD has been shown by careful numerical [19, 24] and analytical studies [25] to be capable of reproducing arbitrary flow fields derived from conventional sharp-interface methods as the viscosity ratio tends to be large enough and the interface thickness tends to be small enough.

Governing equations for mFSI in two-phase flows –

To demonstrate the capability of the DRD approach in simulating mFSI, we consider an immiscible two-phase flow with some suspending objects composed of rigid particles over a rigid corrugated solid boundary (see Fig. 1). We use the phase parameter $\phi(\mathbf{r}, t)$ to describe the fluid-fluid interface and it is locally conserved following $\partial_t \phi + \mathbf{v} \cdot \nabla \phi = -\nabla \cdot \mathbf{J}$, with \mathbf{v} denoting the flow velocity and \mathbf{J} being the diffusion flux. We use the phase parameters $\psi_\alpha(\mathbf{r}; \mathbf{R}_\alpha(t))$ and $\psi(\mathbf{r})$ that both take the form of

Eq. (1) to describe the surface of α -th particle (located at $\mathbf{R}_\alpha(t)$) and the corrugated solid surface, respectively. Then, the governing dynamic equations can be derived using Onsager's variational principle [23, 26–29]. The Rayleighian is given by

$$\mathcal{R}[\mathbf{v}, \mathbf{J}] = \dot{\mathcal{F}} + \Phi - \sum_{\alpha} \mathbf{F}_{\alpha}^{\text{tot}} \dot{\mathbf{R}}_{\alpha} - \int d\mathbf{r} p \nabla \cdot \mathbf{v}, \quad (3)$$

with p being the pressure, a Lagrange multiplier for the local constraint of incompressibility $\nabla \cdot \mathbf{v} = 0$. Here Φ is the dissipation function

$$\Phi[\mathbf{v}, \mathbf{J}] = \int d\mathbf{r} \left[\frac{1}{4} \eta (\nabla \mathbf{v} + \nabla \mathbf{v}^T)^2 + \frac{\mathbf{J}^2}{2M} \right], \quad (4)$$

with T denoting the tensor transpose, and the two resistance coefficients η and M^{-1} being the viscosity and the inverse of mobility, respectively. Physically, the quadratic form of Φ is equivalent to Onsager's linear force-flux relations [22]. \mathcal{F} is the change rate of total free energy \mathcal{F} , given by

$$\mathcal{F} = \mathcal{F}_b[\phi(\mathbf{r})] + \mathcal{F}_s[\phi(\mathbf{r}), \psi(\mathbf{r}), \psi_{\alpha}(\mathbf{r}; \mathbf{R}_{\alpha})]. \quad (5)$$

Here the fluid-bulk energy \mathcal{F}_b is given by $\mathcal{F}_b = \int d\mathbf{r} [f_b(\phi) + \sum_{\alpha} \frac{K}{2} (1 - \psi)(1 - \psi_{\alpha}) |\nabla \phi|^2]$ with $f_b(\phi) = \frac{a}{4} (\phi^2 - 1)^2$ and $\phi = \pm 1$ representing the two fluid phases. The energy parameter a and the interfacial stiffness K are both positive constant. The thickness and interfacial tension of the fluid-fluid interface are given by $\epsilon = \sqrt{K/a}$ and $\gamma = 2\sqrt{2}a\epsilon/3$, respectively. The fluid-solid interfacial energy \mathcal{F}_s is given by $\mathcal{F}_s = \int d\mathbf{r} [\epsilon f_s(\phi) (\sum_{\alpha} |\nabla \psi_{\alpha}|^2 + |\nabla \psi|^2)]$ with $f_s(\phi) = -\frac{1}{4} \gamma \cos \theta_s (\phi^3 - 3\phi)$ being the surface energy density and θ_s being the static contact angle at the solid surfaces.

Minimizing \mathcal{R} with respect to the rates \mathbf{v} and \mathbf{J} gives a set of thermodynamically-consistent dynamic equations:

$$\rho \dot{\mathbf{v}} = -\nabla p + \nabla \cdot [\eta (\nabla \mathbf{v} + \nabla \mathbf{v}^T)] + \hat{\mu}_T \nabla \phi + \mathbf{f}_{\text{tot}}, \quad (6a)$$

$$\dot{\phi} = \nabla \cdot (M \nabla \hat{\mu}_T). \quad (6b)$$

Note that the particle velocity $\dot{\mathbf{R}}_{\alpha}$ is not an independent rate [19] but is slaved by flow field via $\dot{\mathbf{R}}_{\alpha} = \int d\mathbf{r} \psi_{\alpha} \mathbf{v} / \int d\mathbf{r} \psi_{\alpha}$. Here, in Eqs. (6), the dot denotes the material time derivative, ρ is the fluid mass density, $\mathbf{f}_{\text{tot}} = \sum_{\alpha} \psi_{\alpha} \mathbf{F}_{\alpha}^{\text{tot}} / \int d\mathbf{r} \psi_{\alpha}$ is the total force density due to forces $\mathbf{F}_{\alpha}^{\text{tot}}$ applied externally or by other particles on each particle, and $\hat{\mu}_T = \delta \mathcal{F} / \delta \phi$ is the total chemical potential (see Eq. (S17) [23]). The viscosity η and mobility M interpolate smoothly over different domains using either form of Eq. (2) and Eq. (S5) [23], where the solid viscosity η_s is very large and the solid mobility M_s is very small in comparison to those in fluids, *i.e.*, $\eta_s \gg \eta_f$ and

$M_s \ll M_f$. Here three major dimensionless parameters arise: Reynolds number, $\text{Re} \equiv \rho H V_0 / \eta_f$, relative motility parameter, $\mathcal{M} = M_f a / H V_0$, and relative interaction parameter, $\mathcal{A} = a H / \eta_f V_0$ with V_0 being some characteristic velocity. In our simulations, we integrated the dynamic equations (6) in two dimensions (2D) using the finite difference method on staggered grids [30].

In comparison to other DNS methods for mFSI in two-phase flows [1–3], in the DRD approach, proper dynamic boundary conditions at fluid-solid interfaces are imposed by simple smooth interpolations of resistance coefficients (herein, the viscosity η and the mobility M) over various fluid and solid domains. Importantly, classical boundary conditions (such as fluid-impermeability condition, no-slip condition, Navier-slip condition, generalized-Navier-slip condition, and dynamic contact-angle-hysteresis condition) can all be reproduced in the DRD approach as proven by the analysis of sharp-interface limit [23]. Furthermore, since the bulk equations and boundary conditions are derived simultaneously from Onsager's variational principle, thermodynamic consistency is ensured and no further considerations are needed. Next, we present three applications of the DRD approach to mFSI problems taken from different fields.

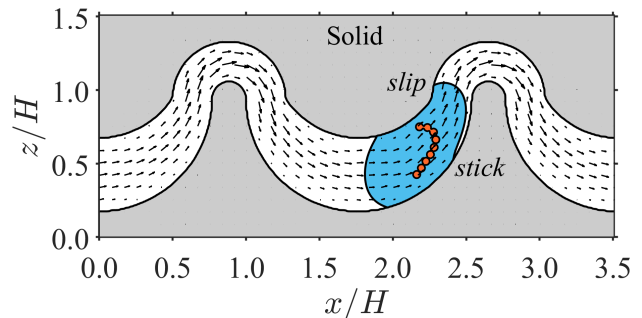


FIG. 2. (Color online) Applications in microfluidics: Transport of a droplet containing a flexible fiber in a corrugated microchannel. A snapshot of the whole computational domain is shown and the contact lines show a stick-slip motion. Here inlet/outlet conditions apply at the two channel-ends and we take $\text{Re} = 1.0$, $\mathcal{M} = 10.0$, $\mathcal{A} = 2000.0$, $\epsilon_s/H = 0.01$, $\eta_s/\eta_f = 100$, and $M_s/M_f = 0$; the fiber stretching and bending stiffness parameters, $\mathcal{K}_s = 5.0$ and $\mathcal{K}_b = 0.25$, with static contact angle 135° and 90° at the channel and the fiber surfaces, respectively.

Applications in microfluidics – In microfluidics, researchers focus on manipulating and controlling fluids in channels at microscales [1]. DNS provides detailed insights into fluid behaviors that are crucial for advancing microfluidic technologies and applications. However, many significant challenges have been posed to the DNS of mFSI in microfluidics due to the complex interactions between different fluid phases and the confined complex geometries involved.

To demonstrate the validity and power of the DRD approach in overcoming these challenges, we first carried out benchmark simulations of inertial particle focusing in 2D microchannels with planar and corrugated surfaces [23]. The results agree well with those obtained from other DNS methods [31] (see Figs. S5 and S6 [23]). Moreover, we have simulated the equilibrating dynamics of a sessile droplet on planar solid surfaces with various contact angles (see Figs. S10 [23]). After that, we simulated a typical process in microfluidics: the transport of a droplet with a suspending flexible fiber in an asymmetrically curved microchannel (see Fig. 2). Interestingly, we observed a stick-slip motion of the droplet contact lines on the microchannel surfaces, which can be attributed to the strong dependence of effective slip length on the local curvature of the corrugated microchannel. It has been predicted before [32] that fluid slip is enhanced (or suppressed) by concave (or convex) surfaces. Therefore, one would expect the contact lines to slip when moving from convex to concave surfaces and stick when moving in turn from concave to convex surfaces (see Fig. 2).

Applications in active matter hydrodynamics – Active matter dynamics refers to the collective behaviors exhibited by self-propelled entities, such as bacteria, cells, or synthetic micro-robots, that interact with their environment [33]. For hydrodynamic behaviors of active matter, DNS provides valuable insights into the underlying mechanisms that are essential for understanding living matter systems and designing active matter-based technologies.

To apply the DRD approach to simulate mFSI in active matter, we first validated the DRD approach by simulating and confirming the far-field dipolar flow field generated by a dumbbell model microswimmer [34] (see Figs. S8 [23]). We then simulated the interaction of 40 dumbbell microswimmers (with a volume fraction 8%) with a fairly flexible (passive) fiber composed of 15 rigid beads (see Fig. 3). Two types of simulations have been carried out: (i) DRD (wet) simulations with hydrodynamic interactions (HIs) and (ii) Brownian (dry) dynamics simulations without HIs, to unveil the effects of HIs on the emergent dynamics of the fiber. In Fig. 3(a), we observed the emergence of a turbulent-like flow pattern in the suspension of self-propelling microswimmers; the fiber is deformed significantly but quite differently from that in dry active baths, highlighting the potential significance of HIs. Moreover, the effects of HIs can be further recognized by tracking the center-of-mass of the fiber and comparing its mean-square-displacement (MSD) in wet microswimmer baths with those in dry active baths, as shown in Fig. 3(b). The diffusion of the fiber is superdiffusive in the wet bath of microswimmers with HIs, while it is normally diffusive (Brownian) for the fiber immersed in the dry active bath without HIs [35].

Applications in reactive porous-media flows – The DRD approach can also be applied to study mFSI that involve the evolution of solid surfaces due to phase tran-

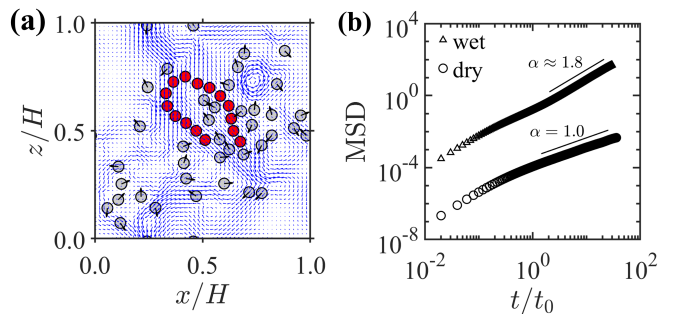


FIG. 3. (Color online) Applications in active matter hydrodynamics: Dynamics of a flexible fiber suspending in a bath of microswimmer suspension. (a) Snapshot of the computational domain is shown. (b) Comparisons of the mean-square-displacement ($\text{MSD} \propto t^\alpha$) of the center-of-mass of the fiber (superdiffusive, $\alpha > 1$) in wet microswimmer baths with those (normally diffusive, $\alpha = 1$) in dry active baths. Here periodic boundary conditions apply at all directions and we take $\text{Re} = 1.0$, $\text{Pe} = 2.0$, $\eta_s/\eta_f = 50$, $\epsilon_s/H = 0.08$, the reduced bead diameters $r_d = d/H = 0.05$; the fiber stretching and bending stiffness parameters: $\mathcal{K}_s = 5.0$ and $\mathcal{K}_b = 0.25$; t_0 to be 10 times persistence time.

sitions or chemical reactions such as porous-media flows involving surface precipitation or dissolution [21]. In this case, DNS at microscopic pore scales can provide detailed insights into the complex interplay among multiphase flow patterns, capillary forces, transport processes, the impact of pore-scale heterogeneities, and fluid-solid phase transitions. This knowledge is crucial for various applications [36], including filtration processes and microbially/enzyme-induced Calcite precipitation (MICP/EICP) for soil stabilization, enabling the design of sustainable porous-media systems and the optimization of MICP/EICP performance.

As an example, we consider a porous-media flow that couples with solute diffusion in the fluid bulk and solute precipitation & dissolution that is assumed, for simplicity, to occur only at solid surfaces [36]. In this case, the fluid is a single-phase solution with diffusing solutes of concentration c , while the solute concentration in the solid is kept constant c_s and the structure or shape of the solid evolves with time. The fluid-solid interface is described by ψ given in Eq. (1) and evolves with a velocity $V_{\text{int}} = r_p/c_s$ that is determined by transition kinetics at the interfaces with r_p denoting the net precipitation rate. To model the evolution of ψ , we have several choices [14, 15]. We can prescribe ψ based on the interface positions obtained by V_{int} ; this, however, is problematic when interfaces break or coalesce. Alternatively and more generally, we can solve the Hamilton-Jacobi equation or the advective Cahn-Hilliard equation for ψ [14].

The Rayleighian takes the form of $\mathcal{R}[\mathbf{v}, \mathbf{J}, r_p] = \dot{\mathcal{F}} + \Phi_T - \int dr p \nabla \cdot \mathbf{v}$, where the total dissipation function is $\Phi_T[\mathbf{v}, \mathbf{J}, r_p] = \Phi[\mathbf{v}, \mathbf{J}] + \int dr [\frac{1}{2} \Gamma^{-1} r_p^2 |\nabla \psi(\mathbf{r}, t)|^2]$ with Φ given in Eq. (4), $M = cD/k_B T$, D being the solute dif-

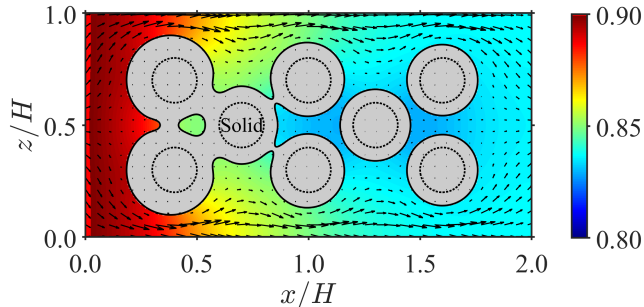


FIG. 4. (Color online) Applications in reactive porous-media flows with precipitation at solid surfaces (of initial solid volume fraction 13%). A snapshot is taken for the whole computational domain including the flow field (arrows), the concentration field (color), and the evolved porous structure (gray) that is composed initially of a hexagonal lattice of cylinders (dashed lines, of diameter $0.2H$). Here periodic boundary conditions and inlet/outlet conditions apply in the vertical and horizontal directions, respectively, and we take $Re = 2.7$, $Pe = Da = 1.0$, $c_{eq}/c_s = 0.8$; the inlet concentration $c_0/c_s = 0.9$, $\epsilon_s/H = 0.01$, $\eta_s/\eta_f = 100$, and $D_s/D_f = 0$.

fusivity, and $k_B T$ being the product of the Boltzmann constant and the temperature. The free energy is given by $\mathcal{F} = \int d\mathbf{r} [f(c) + \psi f_{ss}(c_s)]$ with $f(c) = k_B T c \ln c$ and f_{ss} being the energy density of the solid phase. Minimizing \mathcal{R} gives Eq. (6a) (taking $\phi = 0$ and $\mathbf{f}_{tot} = 0$),

$$\dot{c} = \nabla \cdot (D \nabla c) - r_p (1 - c/c_s) |\nabla \psi(\mathbf{r}, t)|, \quad (7a)$$

$$r_p = k_r (c^2/c_{eq}^2 - 1), \quad (7b)$$

with k_r being a (positive) constant reaction rate [37] and $c_{eq} (< c_s)$ being the equilibrium concentration. Here the smooth interpolations of viscosity $\eta(\mathbf{r})$ and diffusivity $D(\mathbf{r})$ both take the form of Eq. (2). A very large viscosity $\eta_s (\gg \eta_f)$ and very small diffusivity $D_s (\ll D_f)$ in the solid domain can reproduce the following boundary conditions in the sharp interface limit [23]: $\mathbf{v} = \mathbf{0}$ and $\hat{\mathbf{n}} \cdot D_f \nabla c = r_p (1 - c/c_s)$ with $\hat{\mathbf{n}}$ being the outward surface unit normal vector. Three major dimensionless parameters arise: Reynolds number, $Re \equiv \rho H k_r / \eta_f c_s$, Péclet number, $Pe \equiv V_0 H / D_f$ with V_0 being the maximum inlet velocity, and Damköhler number, $Da \equiv H k_r / D_f c_s$. Using the same algorithm as before, we integrated the dynamic equations (6a) and (7) in 2D using the finite difference method on staggered grids [30].

We first validated the DRD approach by simulating precipitation dynamics in 1D [23]. The numerical solutions are found to agree quantitatively with those of sharp interface models in a large range of $Da \in [0.01, 1000]$ (see Fig. S11 [23]). We then simulated a single-phase flow passing through a porous-media initially composed of a hexagonal lattice of cylinders (nucleates) where viscous flows are coupled with solute diffusion

in the bulk and precipitation at the solid surfaces (see Fig. 4). We found that some holes are formed and the highly heterogeneous porous structure can be controlled and manipulated by tuning the competing transport phenomena through dimensionless parameters. Further DNS explorations of this system would help to optimize important engineering processes such as MICP/EICP.

In summary, we propose and validate a generic monolithic DNS approach (DRD) for mFSI in multicomponent multiphase flows that are ubiquitous in nature and modern engineering processes. It provides a natural way of overcoming major challenges in simulating mFSI. The DRD approach can be further extended (*e.g.*, by combining with deformable particle model [38] and dynamic van der Waas theory [39]) to simulate more complex mFSI that involves multiphysics multi-field couplings, *e.g.*, viscoelastic fluids, deformable elastic solids, external electric or magnetic fields, two-phase fluids in heat flow and/or involving phase transitions, thermal fluctuations, and biological activities. Such a generic efficient DNS approach for mFSI provides a promising tool to unveil fundamental physical mechanisms in complex mFSI, perform precise control of microscale fluids, and optimize engineering processes in applications such as microfluidics, additive manufacturing, and biomedical engineering where the technology bottleneck usually arises from ultra-high-dimensional parameter space and high trial-and-error costs.

We thank Tiezheng Qian, Xiao-Ping Wang, Dong Wang, Haiqin Wang, Yanan Liu, and Guangyin Jing for some useful discussions and comments. X. Xu is supported partly by the National Natural Science Foundation of China (NSFC, No. 12131010). The numerical computations were performed on TianHe-2 through the Shanxi Supercomputing Center of China. M. Gao and Z. Li contributed equally to this work.

* Corresponding authors; xu.xinpeng@gtiit.edu.cn

- [1] B. J. Kirby, *Micro-and nanoscale fluid mechanics: transport in microfluidic devices* (Cambridge university press, 2010).
- [2] S. Subramaniam, Multiphase flows: Rich physics, challenging theory, and big simulations, *Physical Review Fluids* **5**, 110520 (2020).
- [3] G. Hou, J. Wang, and A. Layton, Numerical methods for fluid-structure interaction—a review, *Commun. Comput. Phys.* **12**, 337 (2012).
- [4] E. H. Dowell and K. C. Hall, Modeling of fluid-structure interaction, *Annual review of fluid mechanics* **33**, 445 (2001).
- [5] B. E. Griffith and N. A. Patankar, Immersed methods for fluid-structure interaction, *Annual review of fluid mechanics* **52**, 421 (2020).
- [6] Z.-G. Feng and E. E. Michaelides, Heat transfer in particulate flows with direct numerical simulation (dns), In-

- ternational Journal of Heat and Mass Transfer **52**, 777 (2009).
- [7] M. S. Shadloo, G. Oger, and D. Le Touzé, Smoothed particle hydrodynamics method for fluid flows, towards industrial applications: Motivations, current state, and challenges, *Computers & Fluids* **136**, 11 (2016).
- [8] P. Hoogerbrugge and J. Koelman, Simulating microscopic hydrodynamic phenomena with dissipative particle dynamics, *Europhysics letters* **19**, 155 (1992).
- [9] J. T. Padding and A. A. Louis, Hydrodynamic and brownian fluctuations in sedimenting suspensions, *Phys. Rev. Lett.* **93**, 220601 (2004).
- [10] J. Brannick, C. Liu, T. Qian, and H. Sun, Diffuse interface methods for multiple phase materials: an energetic variational approach, *Numer. Math.-Theory Mes.* **8**, 220 (2015).
- [11] D. Mokbel, H. Abels, and S. Aland, A phase-field model for fluid–structure interaction, *Journal of Computational Physics* **372**, 823 (2018).
- [12] J. Yang and J. Kim, A phase-field method for two-phase fluid flow in arbitrary domains, *Comput. Math. Appl.* **79**, 1857 (2020).
- [13] R. Glowinski, T.-W. Pan, T. I. Hesla, D. D. Joseph, and J. Periaux, A fictitious domain approach to the direct numerical simulation of incompressible viscous flow past moving rigid bodies: application to particulate flow, *Journal of computational physics* **169**, 363 (2001).
- [14] X. Li, J. Lowengrub, A. Rätz, and A. Voigt, Solving pdes in complex geometries: a diffuse domain approach, *Communications in mathematical sciences* **7**, 81 (2009).
- [15] Z. Guo, F. Yu, P. Lin, S. Wise, and J. Lowengrub, A diffuse domain method for two-phase flows with large density ratio in complex geometries, *Journal of Fluid Mechanics* **907**, A38 (2021).
- [16] Y. Nakayama and R. Yamamoto, Simulation method to resolve hydrodynamic interactions in colloidal dispersions, *Physical Review E* **71**, 036707 (2005).
- [17] R. Yamamoto, J. J. Molina, and Y. Nakayama, Smoothed profile method for direct numerical simulations of hydrodynamically interacting particles, *Soft Matter* **17**, 4226 (2021).
- [18] H. Tanaka and T. Araki, Simulation method of colloidal suspensions with hydrodynamic interactions: Fluid particle dynamics, *Phys. Rev. Lett.* **85**, 1338 (2000).
- [19] A. Furukawa, M. Tateno, and H. Tanaka, Physical foundation of the fluid particle dynamics method for colloid dynamics simulation, *Soft Matter* **14**, 3738 (2018).
- [20] A. De Rosis, G. Falcucci, S. Ubertini, F. Ubertini, and S. Succi, Lattice boltzmann analysis of fluid-structure interaction with moving boundaries, *Communications in Computational Physics* **13**, 823 (2013).
- [21] A. J. Ladd and P. Szymczak, Reactive flows in porous media: challenges in theoretical and numerical methods, *Annual review of chemical and biomolecular engineering* **12**, 543 (2021).
- [22] L. Onsager, Reciprocal relations in irreversible processes. i., *Phys. Rev.* **37**, 405 (1931).
- [23] See the Supplementary Information [url].
- [24] J. Su, K. Ma, Z. Yan, Q. He, and X. Xu, Dynamics of flexible fibers in confined shear flows at finite reynolds numbers, *Phys. Fluids* **35** (2023).
- [25] Y. Fujitani, Connection of fields across the interface in the fluid particle dynamics method for colloidal dispersions, *J. Phys. Soc. Japan* **76**, 064401 (2007).
- [26] T. Qian, X.-P. Wang, and P. Sheng, A variational approach to moving contact line hydrodynamics, *J. Fluid Mech.* **564**, 333 (2006).
- [27] M. Doi, Onsager principle in polymer dynamics, *Prog. Polym. Sci.* **112**, 101339 (2021).
- [28] H. Wang, T. Qian, and X. Xu, Onsager’s variational principle in active soft matter, *Soft Matter* **17**, 3634 (2021).
- [29] H. Wang, B. Zou, J. Su, D. Wang, and X. Xu, Variational methods and deep ritz method for active elastic solids, *Soft Matter* **18**, 6015 (2022).
- [30] M. Gao and X.-P. Wang, An efficient scheme for a phase field model for the moving contact line problem with variable density and viscosity, *Journal of Computational Physics* **272**, 704 (2014).
- [31] D. V. Esipov, D. V. Chirkov, D. S. Kuranakov, and V. N. Lapin, Direct numerical simulation of the segre–silberberg effect using immersed boundary method, *Journal of Fluids Engineering* **142**, 111501 (2020).
- [32] D. Einzel, P. Panzer, and M. Liu, Boundary condition for fluid flow: curved or rough surfaces, *Phys. Rev. Lett.* **64**, 2269 (1990).
- [33] M. C. Marchetti, J.-F. Joanny, S. Ramaswamy, T. B. Liverpool, J. Prost, M. Rao, and R. A. Simha, Hydrodynamics of soft active matter, *Rev. Mod. Phys.* **85**, 1143 (2013).
- [34] A. Furukawa, D. Marenduzzo, and M. E. Cates, Activity-induced clustering in model dumbbell swimmers: the role of hydrodynamic interactions, *Phys. Rev. E* **90**, 022303 (2014).
- [35] N. Nikola, A. P. Solon, M. Kardar, J. Tailleur, and R. Voituriez, Active particles with soft and curved walls: Equation of state, ratchets, and instabilities, *Phys. Rev. Lett.* **117**, 098001 (2016).
- [36] A. Almajed, M. A. Lateef, A. A. B. Moghal, and K. Lemboye, State-of-the-art review of the applicability and challenges of microbial-induced calcite precipitation (micp) and enzyme-induced calcite precipitation (eicp) techniques for geotechnical and geoenvironmental applications, *Crystals* **11**, 370 (2021).
- [37] T. Van Noorden and I. Pop, A stefan problem modelling crystal dissolution and precipitation, *IMA J. Appl. Math.* **73**, 393 (2008).
- [38] A. Boromand, A. Signoriello, F. Ye, C. S. O’Hern, and M. D. Shattuck, Jamming of deformable polygons, *Phys. Rev. Lett.* **121**, 248003 (2018).
- [39] A. Onuki, Dynamic van der waals theory of two-phase fluids in heat flow, *Phys. Rev. Lett.* **94**, 054501 (2005).